

Modelling retention and dispersion mechanisms of bluefin tuna eggs and larvae in the northwest Mediterranean Sea

Patrizio Mariani^{a,*}, Brian R. MacKenzie^{a,b}, Daniele Iudicone^c, Alexandra Bozec^d

^a Technical University of Denmark, National Institute of Aquatic Resources (DTU Aqua), Charlottenlund Castle, DK-2920 Charlottenlund, Denmark

^b University of Aarhus, Department of Marine Ecology, c/o DTU Aqua, Charlottenlund Castle, DK-2920 Charlottenlund, Denmark

^c Zoological Station of Naples "A. Dohrn", Lab. Biological Oceanography, Italy

^d Florida State University, Center for Ocean-Atmospheric Prediction Studies, USA

ARTICLE INFO

Article history:

Received 28 February 2008

Received in revised form 2 November 2009

Accepted 10 April 2010

Available online 20 April 2010

ABSTRACT

Knowledge of early life history of most fish species in the Mediterranean Sea is sparse and processes affecting their recruitment are poorly understood. This is particularly true for bluefin tuna, *Thunnus thynnus*, even though this species is one of the world's most valued fish species. Here we develop, apply and validate an individually based coupled biological–physical oceanographic model of fish early life history in the Mediterranean Sea. We first validate the general structure of the coupled model with a 12-day Lagrangian drift study of anchovy (*Engraulis encrasicolus*) larvae in the Catalan Sea. The model reproduced the drift and growth of anchovy larvae as they drifted along the Catalan coast and yielded similar patterns as those observed in the field. We then applied the model to investigate transport and retention processes affecting the spatial distribution of bluefin tuna eggs and larvae during 1999–2003, and we compared modelled distributions with available field data collected in 2001 and 2003. Modelled and field distributions generally coincided and were patchy at mesoscales (10s–100s km); larvae were most abundant in eddies and along frontal zones. We also identified probable locations of spawning bluefin tuna using hydrographic backtracking procedures; these locations were situated in a major salinity frontal zone and coincided with distributions of an electronically tagged bluefin tuna and commercial bluefin tuna fishing vessels. Moreover, we hypothesized that mesoscale processes are responsible for the aggregation and dispersion mechanisms in the area and showed that these processes were significantly correlated to atmospheric forcing processes over the NW Mediterranean Sea. Interannual variations in average summer air temperature can reduce the intensity of ocean mesoscale processes in the Balearic area and thus potentially affect bluefin tuna larvae. These modelling approaches can increase understanding of bluefin tuna recruitment processes and eventually contribute to management of bluefin tuna fisheries.

© 2010 Elsevier Ltd. All rights reserved.

1. Introduction

The North Atlantic bluefin tuna (*Thunnus thynnus thynnus*, Linnaeus, 1758) is a large, highly migratory pelagic predator whose historical range encompasses the shelf and open sea areas of the North Atlantic, the Mediterranean Sea and the Black Sea (Mather et al., 1995; Fromentin and Powers, 2005). The species spawns in spring and summer in the Gulf of Mexico and Mediterranean Sea, after which adults migrate north for feeding (Mather et al., 1995; Cury et al., 1998). Major fisheries on bluefin tuna have existed for centuries but, despite the high economic importance of these fisheries, there are still major gaps in knowledge of bluefin tuna ecology (Fromentin and Powers, 2005).

Some of the largest gaps relate to recruitment and oceanographic processes affecting survival of the early life stages. For example, in the Mediterranean Sea some spawning areas were identified decades ago (e.g. near the Balearic Islands and Sicily; Mather et al., 1995; Fromentin and Powers, 2005), but others have only recently been identified (e.g. near Cyprus; Karakulak et al., 2004), while the presence of spawning in other areas may vary over time and is not well documented (e.g. the Adriatic Sea; Mather et al., 1995; Fromentin and Powers, 2005). In different locations, the survival probability of eggs and larvae is not known and could vary both within and among years possibly as a response to spatial and temporal variability in different environmental conditions.

To improve knowledge of the early life history of bluefin tuna and how it is influenced by environmental conditions, comprehensive field investigations have been conducted since 2001 around the Balearic Islands, northwest Mediterranean Sea (Alemany et al., 2006; Garcia et al., 2006b). The spawning habitat for bluefin

* Corresponding author. Address: Kavalergården 6, DK-2920 Charlottenlund, Denmark. Tel.: +45 3396 3353; fax: +45 3396 3434.

E-mail address: pat@aqu.dtu.dk (P. Mariani).

tuna is characterized by the presence of numerous mesoscale oceanographic features that appear to aggregate and retain several larval species (Alemany et al., 2006; Garcia et al., 2006b). These frontal structures seem to concentrate bluefin tuna larvae at restricted spatial scales.

Given that temperatures during the larval production period are relatively high (Mather et al., 1995; Garcia et al., 2006b), bioenergetic demands of larvae for food (i.e. zooplankton) will also be high (Houde, 1989; MacKenzie et al., 1990). However, the Mediterranean Sea is characterized by relatively low levels of plankton production (Agostini and Bakun, 2002; Sabates et al., 2007a); hence, larvae have a bioenergetic requirement for high concentrations of prey in an environment that paradoxically, is relatively unproductive. As a consequence, localized areas with higher prey concentrations and physical processes which can aggregate and retain larvae together with their prey or advect larvae to relatively prey-rich areas, could increase survival probability (Sabates et al., 2007a). In the Mediterranean, mesoscale dynamics (Velez-Belchi and Tinore, 2001) may favor locally elevated plankton production rates (Agostini and Bakun, 2002), or produce “predator refuges” (Bakun, 2006). These phenomena could promote or suppress survival of eggs and larvae produced at different times throughout the year and in different areas.

In this study, we developed and applied an individual-based coupled biological–physical oceanographic model for bluefin tuna larvae around the Balearic Islands (Fig. 1A). We used this model to investigate the spatial, seasonal and interannual variability of egg and larval distributions in this area, and to determine the influence of regional climatic and hydrographic variations on their distributions. Numerical simulations were performed under simple biological constraints in order to identify bluefin tuna spawning grounds and the emerging patterns of aggregation, retention and dispersion of bluefin tuna larvae. We focused in particular on how mesoscale hydrographic activity affects the seasonal and year-to-year variability of spawning and subsequent larval distributions around the Balearic Islands.

However, before applying the model, we tested its numerical structure and performances with a detailed Lagrangian dataset on drift and growth of anchovy larvae collected in the summer of 2000 in the northwest Mediterranean Sea (Sabates et al., 2007b).

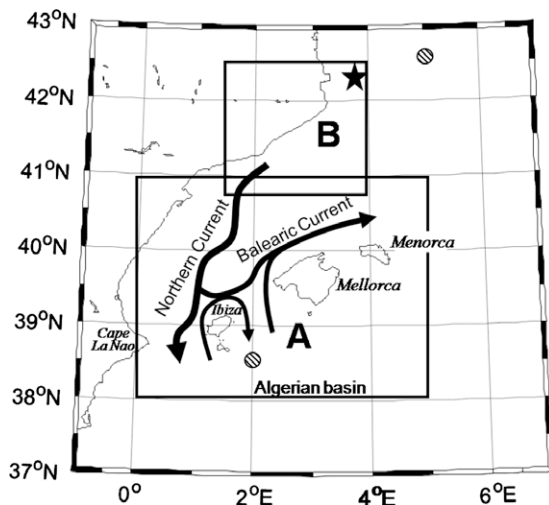


Fig. 1. Map of the area examined for (A) the bluefin tuna and (B) anchovy distributions. The star, ★ represents the site of release of larvae in the anchovy tracking experiment, while the two circles are the locations where atmospheric forcing data were extracted for analysis.

2. Materials and methods

2.1. Geographic and oceanographic context

The area investigated for bluefin tuna distribution is located around the Balearic Islands and included the Balearic Sea in the North, the Algerian Basin in the South (Fig. 1A), and it is open in the north to the Catalan Sea (Fig. 1A and B). The Balearic Sea is characterized by cooler and more saline waters than the Algerian Basin, where warmer and fresher waters of Atlantic origins are present (Pinot et al., 2002). Northern and southern regions are connected by the presence of the Balearic Channels: Ibiza Channel, Mallorca Channel and Menorca Channel. The Ibiza Channel corresponds to the 80-km wide (at the surface) and 800-m deep passage intersecting the Balearic topographic ridge between Ibiza and the Iberia peninsula at Cape La Nao. The passage between Ibiza and Mallorca, the Mallorca Channel, is a shallow sill with a 500-m depth, while the Menorca Channel is the shallow (<200 m) passage between Mallorca and Menorca (Pinot et al., 2002).

The area is characterized by several front and eddy structures related to strong mesoscale activity generated at the interface between different water masses of Atlantic (AW) and Mediterranean (MW) origins (e.g. Pinot et al., 2002). The average circulation in the area is strongly affected by the Northern Current flowing south-westward into the Balearic Sea (Fig. 1). Close to the Ibiza channel this current splits and one branch proceeds southward mixing into the Algerian Basin with the warmer and fresher Atlantic water, while a minor portion forms the Balearic Current that is also reinforced by water flowing northward through the Mallorca Channel (Astraldi and Gasparini, 1992). This average climatological circulation and associated fronts are, however, highly variable on a year-to-year and seasonal temporal scale (Pinot et al., 2002).

2.2. Hydrodynamic model

The hydrodynamic model used in this work is an implementation of the Ocean General Circulation Model – OPA – in the Mediterranean Sea (Madec et al., 1998). The OPA is a general ocean circulation model that solves the primitive equation under hydrostatic and Boussinesq approximations. Small-scale mixing processes are parameterized with a bi-Laplacian formulation of the horizontal eddy viscosity and diffusivity, and a 1.5 turbulence closure scheme for the vertical components (Blanke and Delecluse, 1993).

The system of partial differential equations are solved on a numerical grid with resolution of $1/8^\circ$ extending from 29°N to 46°N in latitude and from 12°W to 38°E in longitude including the Mediterranean Sea and part of the Atlantic Ocean. The vertical grid has 43 levels with spacing varying from 6 m in the surface, up to 200 m in depth with partial step parameterization for the bathymetry (Pacanowski and Gnanadesikan, 1998). Daily high-resolution wind stress and air-sea fluxes provided by ECMWF (European Centre for Medium-Range Weather Forecast; $0.5^\circ \times 0.5^\circ$) and monthly climatology of 31 major river runoffs are used to force the model, while initial temperature and salinity fields are derived from the MEDATLAS II monthly climatology. Relaxation of salinity and temperature towards climatological values are used to model the exchanges in the Gibraltar area between Atlantic and Mediterranean waters (Bozec et al., 2006).

This state-of-the-art eddy-permitting configuration of OPA is able to well reproduce major patterns of the surface and thermohaline circulation in the Mediterranean Sea (Bozec et al., 2006). At the surface, the anti-estuarine circulation is well reproduced with the presence of the Alboran Gyre (Vargas-Yañez et al., 2000) and the penetration of the Atlantic Waters in the western basin through

the Algerian current. The flow separates into two branches at the Sicily Strait (Astraldi et al., 2002): one passes through the strait while the other flows north in the Tyrrhenian Sea toward the Corsica Strait and finally feeds the Liguro-Provençal Current (Millot, 1999). In the eastern basin, we find the Atlantic Ionian Stream flowing eastward to the Levantine Basin (Robinson et al., 1999) and finally joining the cyclonic coastal circulation of the sub-basin (Alhammoud et al., 2005). The thermohaline circulation is also correctly represented during the simulation with deep and intermediate water mass formation in the main convection sites of the Mediterranean Sea: The Gulf of Lion, the Adriatic Sea, the Levantine Basin and the Aegean Sea (MEDOC Group, 1970; Vilibic and Orlic, 2000). The circulation of the model at surface and depth reproduces the observed patterns, and has also been used to determine the impact of the penetrative solar radiation on water mass transformation (Bozec et al., 2008).

Hydrodynamic fields (temperature, salinity, currents and diffusivity) have been stored every 5 days from 1999 to 2003 and this dataset was then used for the analyses of fish larvae dispersion.

2.3. Individual-based model of fish early life stages

Numerical particles representing eggs and fish larvae are moved by a particle tracking scheme that included a corrected random walk to model their positions during the simulated period. The random walk was modified to include a particle displacement term that is a function of the local diffusivity gradient (Visser, 1997). Three-dimensional fields of velocity and vertical diffusivity were extracted from the archived hydrodynamic simulations and interpolated to the particle positions in order to obtain the deterministic and the stochastic component of the model. These interpolations were performed with a bi-linear interpolation scheme on the horizontal while, to reduce numerical artifacts (Ross and Sharples, 2004; North et al., 2006), a smoothing spline algorithm (de Boor, 1978) is used on the vertical. Under the assumption of isotropic turbulence at the scales of the organisms, we use vertical eddy diffusivity to derive stochastic components along both horizontal and vertical directions. Integration in time is performed with a second order Runge–Kutta scheme and time step equal to $dt = 60$ s. All the archived three-dimensional fields from the physical model, which were stored at 5 days interval, were then linearly interpolated to match this shorter time step.

Eggs are neutrally buoyant passive moving particles and after a given period of time they switch into a larval stage where a behavioral swimming component is included in the model – typically one body length per second and in a random direction. Larvae are assumed to grow in length as a function of age (bluefin tuna simulations) and temperature (anchovy simulations) while no mortality terms have been parameterized. Temperature is interpolated with a tri-linear interpolation scheme to the particle positions.

We tested our particle-tracking algorithm with several 1D and 2D test cases using passive moving particles (no swimming component) in order to verify the robustness of the model under both stationary and varying hydrographic conditions. For the values of diffusivity gradients found in the upper layers of the Balearic area (<35-m depth) our model always satisfies the well-mixed criteria showing uniform particles' concentration on the vertical when no other processes were included.

2.4. Identification of drift patterns: aggregation, retention and dispersion

To provide information about the patterns of retention, dispersion and aggregation of eggs and fish larvae, a Eulerian grid at resolution of $1/24^\circ$ was nested into the OPA grid in the area of the

initial particles release. This grid was then used to derive all the statistics on particle dispersion processes.

We first estimated the expected number of particles per grid cell as $\bar{c} = N_0/B$, where B = the total number of grid cells in the nested grid, and N_0 = the number of particles released when the simulation starts. The particle concentration in each grid box is a fluctuating quantity $c_{ij}(t)$, where i and j are the indexes to the specific cell of the nested grid. This quantity can be used to derive an aggregation index estimated as the ratio of $c_{ij}(t)$ and \bar{c} averaged over the simulated period T :

$$\langle C_{ij} \rangle = \frac{T^{-1} \sum_{t=0}^T c_{ij}(t)}{\bar{c}} \quad (1)$$

This index will be >1 where particles aggregate while it will be <1 in the sites where particles disperse.

Furthermore, particles are grouped on the basis of the initial box of release and then, similarly to Hinrichsen et al. (2003b), dispersion and retention were estimated on the nested grid by calculation of simple statistical parameters of particles drift (Fig. 2). Ensemble averaging over individual trajectories of the same group enables calculation of dispersion scales in terms of average distances moved from the point of release (d_{ij}) and in terms of variances of the mean drift distances among particles of the same group (σ_{ij}). The dispersion is then estimated as the root mean square of the variance.

While the aggregation index $\langle C_{ij} \rangle$ is a measure of particles' aggregation, the method above allows discrimination among different dispersion and retention patterns that are relevant for the ecology of the early life stages of fishes. For example, a typical condition of retention is one in which particles do not move far apart from the point of release, i.e. small d_{ij} and low σ_{ij} (Fig. 2a). On the other hand, when particles move for a long distance from the point of release (large d_{ij}) but exhibit a low variability (low σ_{ij}), a different case of retention can be identified by the model (Fig. 2b). Similar arguments can be used for the dispersion patterns with small or large d_{ij} but high σ_{ij} (Fig. 2c and d). The statistical analyses performed with the model output can then provide maps in the given area of emerging patterns of larval aggregation, retention and dispersion as averages over the simulated period.

2.5. Model setup

We conducted several particle-tracking studies for different purposes using anchovy and bluefin tuna larvae (Table 1). To validate the general structure of the model (e.g. tracking algorithm, circulation patterns), we executed a set of numerical experiments using anchovy as a reference species and compared the results with observations collected by Sabates et al. (2007b) along the Catalan coast (Fig. 1B). These authors sampled in June 2000 a parcel of water tracked for 10 days with three surface drifters (10-m deep) launched at the core of the shelf-slope current where low salinity surface waters related to the Rhône River were detected. Hence, this dataset allows us to directly compare the outputs of the model to the observed distribution patterns and the size distribution of anchovies observed on different days.

In the model, anchovy eggs are assumed to hatch 3 ± 0.5 days after release and at an initial length $L_0 = 3.0 \pm 0.3$ mm. Larvae are then followed using a temperature-dependent growth rate $G = 0.06T$ ($^\circ\text{C}$) $- 0.565$ that fits well with available observations on anchovies in different areas (Palomera et al., 2007).

Two sets of experiments were run for anchovies. In the first simulation (*exp01*) we used the model to replicate the positions of the drifters in the tracked water. A group of particles ($\sim 5 \times 10^4$) was then released in a small area (* in Fig. 1B), close

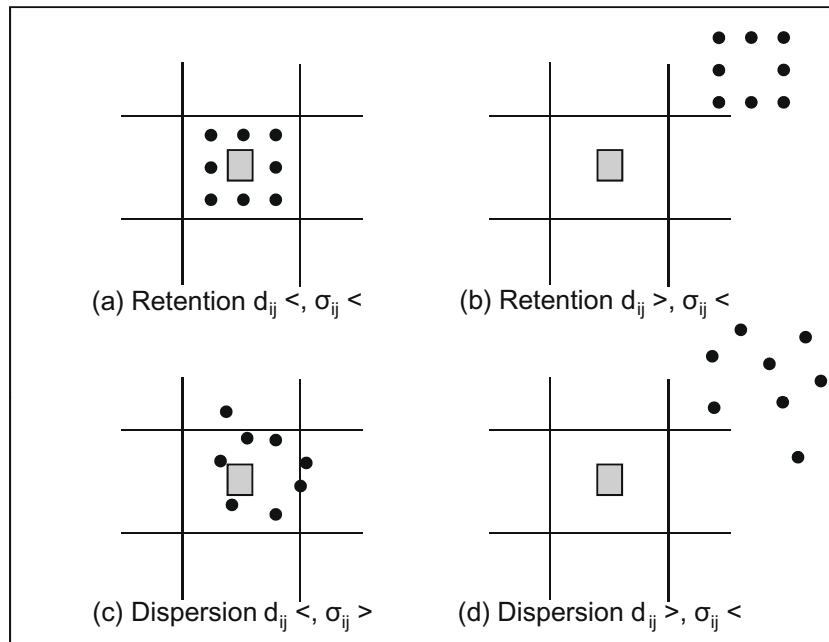


Fig. 2. Retention and dispersion mechanisms analyzed in the model. The large square and small dots respectively indicate the center of spawning areas and larval drifters (after Hinrichsen et al., 2003b). Four cases (a–d) are showed with large (>) and small (<) values in the distance (d_{ij}) and variance (σ_{ij}) over the distances moved by the particles in the box ij .

Table 1

List of numerical simulations performed in this study. Two fish larvae species have been analyzed: bluefin tuna and anchovy, for a total of 29 simulations.

Name	Species	Release	Period	Description
Exp01	Anchovy	1	01/06–13/06, 2000	Single release of 5×10^4 particles in the Rhône River plume followed for 12 day (* in Fig. 1B)
Exp02	Anchovy	1	01/06–13/06, 2000	Single release of 2×10^5 particles in the entire area followed for 15 days (Fig. 1B)
Exp03	Tuna	2	18/06/2001, 08/07/2003	Releases of 2×10^5 particles in the entire Balearic area followed for 20 days (Fig. 1A)
Exp04	Tuna	25	03/06–13/07, 1999–2003	Releases every ten days of 2×10^5 particles in the entire Balearic area followed for 20 days (Fig. 1A)

to the initial position of the experiment of Sabates et al. (2007b) and followed for 12 days.

In the second experiment (*exp02*), a larger group of particles ($\sim 2 \times 10^5$) was uniformly distributed in and off the Catalan continental slope (Fig. 1B) and then their trajectories simulated for 15 days. In both cases, particle positions were constrained to the upper 35 m. At the end of the simulations, the emerging patterns of larval aggregation, retention and dispersion were analyzed as described below for the distribution of bluefin tuna larvae.

A second series of drift modelling simulations analyzed the drift patterns of bluefin tuna eggs and larvae in the Balearic area (Fig. 1A). We released particles on dates which corresponded approximately to the timing of recently published independent ichthyoplankton sampling performed by others (Garcia et al., 2003, 2005a, 2005b, 2006a). Particle release dates were therefore June 18, 2001 and July 8, 2003 (*exp03*, Table 1).

Each release consisted of 2×10^5 egg particles uniformly distributed in the top 35 m of the Balearic area (Fig. 1A). Egg development and larval growth were then followed for 20 days beyond which larval swimming behaviour could potentially dominate hydrographic transport processes (Mather et al., 1995). No vertical migratory behaviour was imposed on the larvae, although the positions of eggs and larvae were constrained to the upper 35 m of the water column by applying reflecting vertical boundary conditions in the model.

Hatching is assumed to occur 2 ± 0.5 days after release and the length at hatch, $L_0 = 2.5 \pm 0.25$ mm (Miyashita et al., 2001). There is little information about growth of bluefin tuna larvae under different temperature conditions; hence, a reliable temperature-dependent growth function cannot be derived. However during 2003–

2005, temperatures were 23.0–27.8 °C and growth rates of larval bluefin tuna in the Balearic area averaged 0.4 mm/day (0.35–0.43, Garcia, pers. comm.). We therefore, assumed that growth rate was constant and similar to that observed, which is also similar for laboratory-reared larval tuna species at similar temperatures (Miyashita et al., 2001; Kawamura et al., 2003; Sawada et al., 2005). Growth rate affects larval length and consequently their swimming velocity. Although differences in swimming velocity can play an important role for the movement of larvae in the vertical, it is assumed that growth-related differences in larval velocity due to temperature will have a relatively small influence on the spatial dispersion of bluefin tuna around the Balearic Islands (see Section 4.3).

Therefore, in summary, several numerical experiments have been performed with the Lagrangian individual-based model described above; the parameters and values used in those experiments are given in Table 1 (see Section 2.6).

2.6. Seasonal and year-to-year variability

A third set of tracking studies investigated the seasonal and interannual variability of bluefin tuna larvae aggregations for a limited number of years (*exp04*). Numerical particles were released every ten days in our model setup between June 3rd and July 13th during 1999–2003 (*exp04*, Table 1).

For each release, we derive the average aggregation value (\bar{C}) as the mean of $\langle C_{ij} \rangle$ in the Balearic area:

$$\bar{C} = \frac{1}{B} \sum_{ij} \langle C_{ij} \rangle \quad (2)$$

Then, a simple index of patchiness (ψ) was calculated at the end of each 20-day simulation:

$$\psi = \frac{\frac{1}{B-1} \sum_{ij} ((C_{ij}) - \bar{C})^2}{C} \quad (3)$$

The equation above is the simple variance over mean ratio and is used to analyze temporal variability of the aggregation patterns over multiple years and multiple releases.

3. Results

3.1. Model evaluation with anchovy larvae distribution

For the sampling period of anchovy larvae (June 2000), the hydrodynamic model predicts a salinity front along the shelf-break of the Catalan coast that separates the relatively low salinity coastal waters from the saltier open ocean waters (Fig. 3a). This front is a semi-permanent feature in the area but observed data (Sabates et al., 2007a) show fresher coastal waters resulting in a salinity gradient stronger than that simulated by the model.

The associated model circulation is generally southward (Fig. 3a). At the north, an intense jet (the Northern Current; Pinot et al., 2002) is simulated offshore while a weaker flow characterizes the shelf area. Farther south, the two current systems become separated by a cyclonic eddy, centered at 3.0°E, 41.12°N. Compared with the observations (Sabates et al., 2007a), this eddy structure

displaced the core of the Northern Current farther south and far from the shelf.

The net southward transport of simulated anchovy eggs and larvae released in the Northern Current (*exp01*) agrees well with observations during most of the simulated period (Fig. 4). However, beginning on day 7 and relative to the drogues, particles move southward slowly and results in a large difference between the drift measured by the drogues and predicted drift locations. This difference is likely due to the weaker circulation of the model and it is almost constant in the following days yielding a net shift of final positions of the particles relative to the drifters (Fig. 4). The mean increase of larval size in the model (0.56 mm/day) is similar to the average growth rate of anchovy larvae observed in the field, i.e. 0.57 mm/day (Sabates et al., 2007b).

The above circulation produces clear patterns in the spatial distribution (retention, aggregation, dispersion) and transport (velocities, distances travelled) of the modelled anchovy larvae (*exp02*; Fig. 3). A coastal to open ocean gradient appears to be present in the average distances moved by the particles suggesting a stronger coastal retention (Fig. 3b). This conclusion is partially confirmed by the aggregation map (Fig. 3c) where modelled anchovy larvae appear to concentrate in the northern part of the area but also off the Catalan coast around 3°E and 41°N, i.e. in the cyclonic eddy described above. The latter is not supported by observations while the aggregation of larvae around 3°30'E, 42°N agrees very well with larvae distribution in the field (Sabates et al., 2007b).

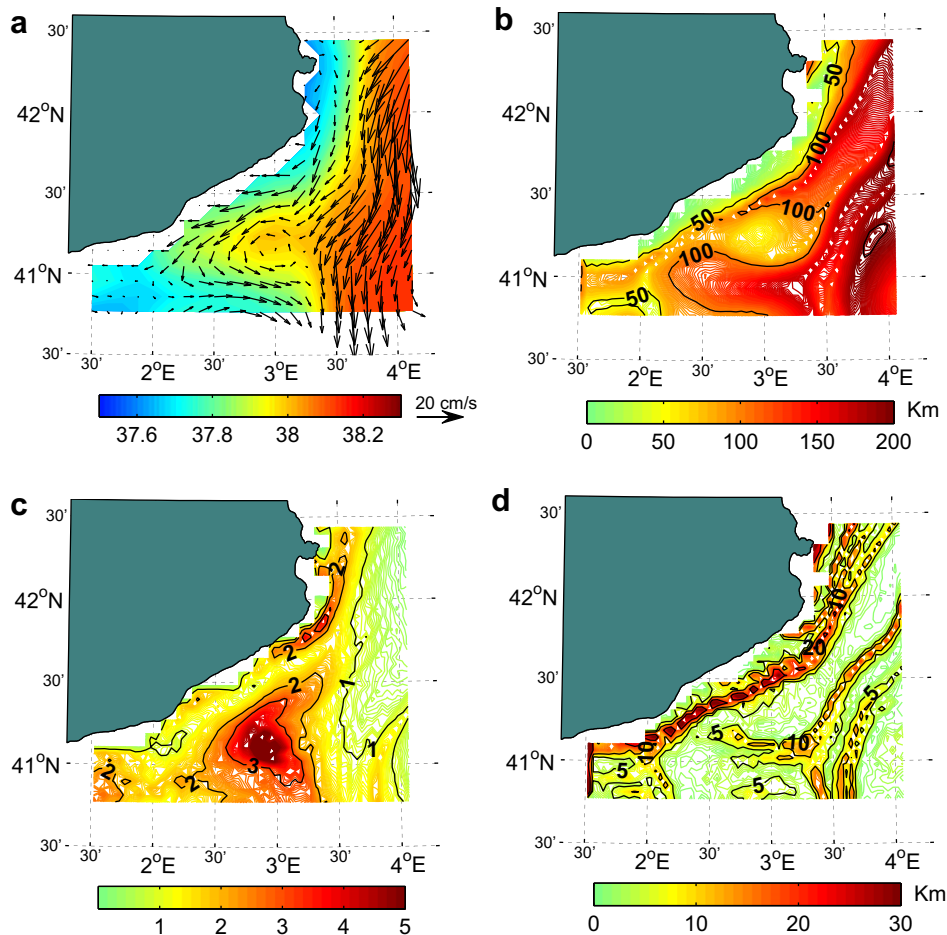


Fig. 3. Modelled ocean circulation and spatial patterns of anchovy larvae in June 2000 in the Catalan Sea area. (a) Velocity and salinity distribution at 35-m depth simulated for the 1st of June 2000. (b) Averaged moved distances, (c) aggregation index and (d) dispersion of modelled anchovy larvae.

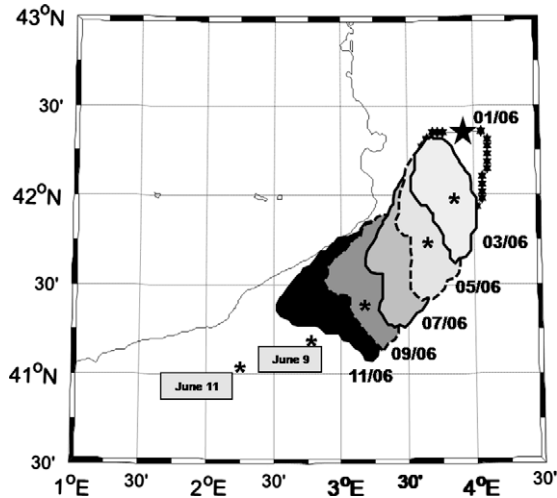


Fig. 4. Particle distributions simulated between the 1st and 11th of June 2000. Data were compared with the positions (*) of the observed Lagrangian drifters.

The dispersion map (Fig. 3d) reveals that particles originating in the coastal region are exposed to a larger variance in the travelled distance than those released offshore. The area of highest variance in travel distance appears to be characterized by the presence of the residual Rhône River plume flowing southwestward along the Catalan coast. This is a boundary region between the coastal area, associated with low velocity, and the offshore region (Fig. 3b). Thus, particles initially very close to each other can have a very different fate depending on if they are trapped along the coast or in the more intense offshore circulation.

We think that the higher dispersion processes shown by these areas can be responsible for the observed strong reduction in the abundances of larvae at day 9 (Sabates et al., 2007b).

3.2. Distribution of bluefin tuna larvae around Balearic Islands

Particles representing bluefin tuna eggs and larvae showed strong spatial variability at mesoscales in their distributional and transport characteristics during both 2001 (Fig. 5) and 2003 (Fig. 6).

In summer 2001, the modelled circulation (Fig. 5a) was characterized by the presence of the Balearic Current flowing northeastward, north of the Balearic Islands and acts as the southern boundary for the salty MW. The current is fed at the Spanish coast by the coastal branch of the Northern Current and reinforced north of Menorca by the conjunction with the southward offshore jet discussed above. South of the Balearic Islands, an eastward meandering jet (velocities are 10–20 cm/s) was associated with the frontal region that bounds the fresher AW. Part of this jet flows anti-cyclonically around Ibiza. The general circulation modelled in 2001 agrees well with the observations collected in the same period by Garcia et al. (2003). The most intense current in the Balearic basin is correctly represented as the current south of the archipelago, and the salinity distribution and mesoscale patterns are also similar. Moreover, both data (Garcia et al., 2003) and simulations present a region of weak currents immediately south of Menorca (Fig. 5a).

In 2001, modelled eggs starting in the southern part of the model domain (Algerian basin) were transported larger distances than those originating in the MW (Fig. 5b). This finding is consistent

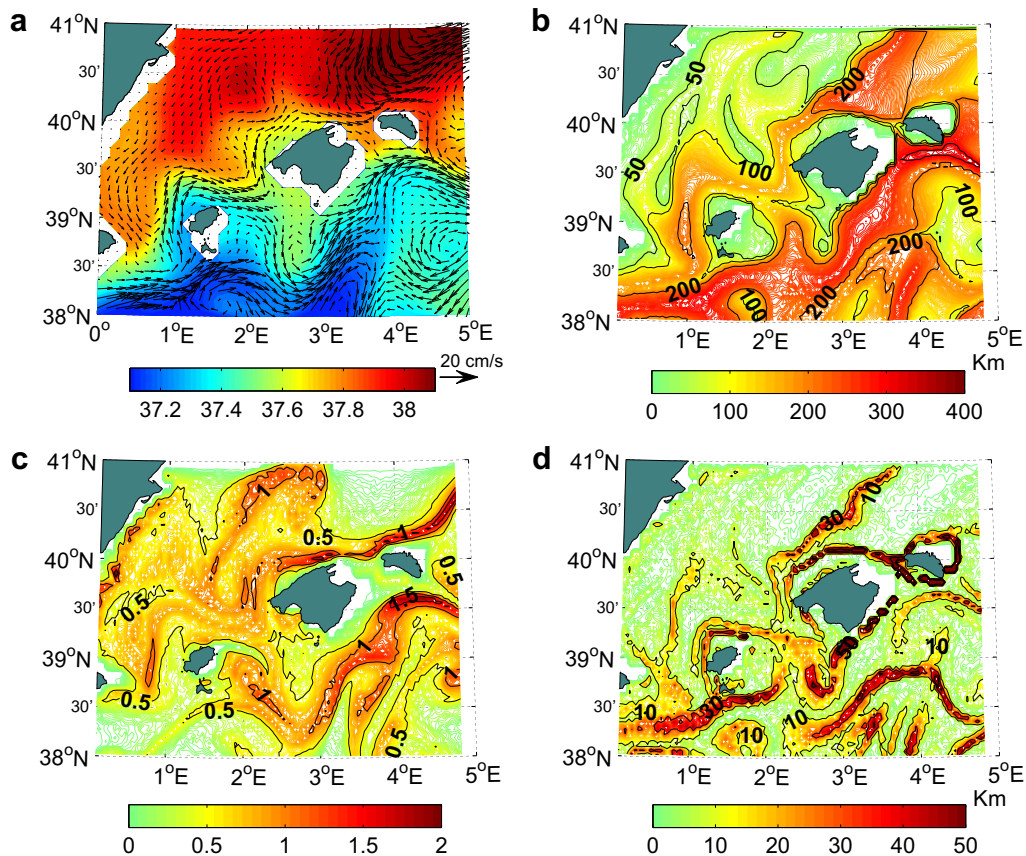


Fig. 5. Modelled ocean circulation and spatial patterns of bluefin tuna larvae in June–July 2001 in the Balearic area. (a) Velocity and salinity distribution at 35-m depth simulated for the 23rd of June 2001. (b) Averaged moved distances, (c) aggregation index and (d) dispersion of modelled bluefin tuna larvae.

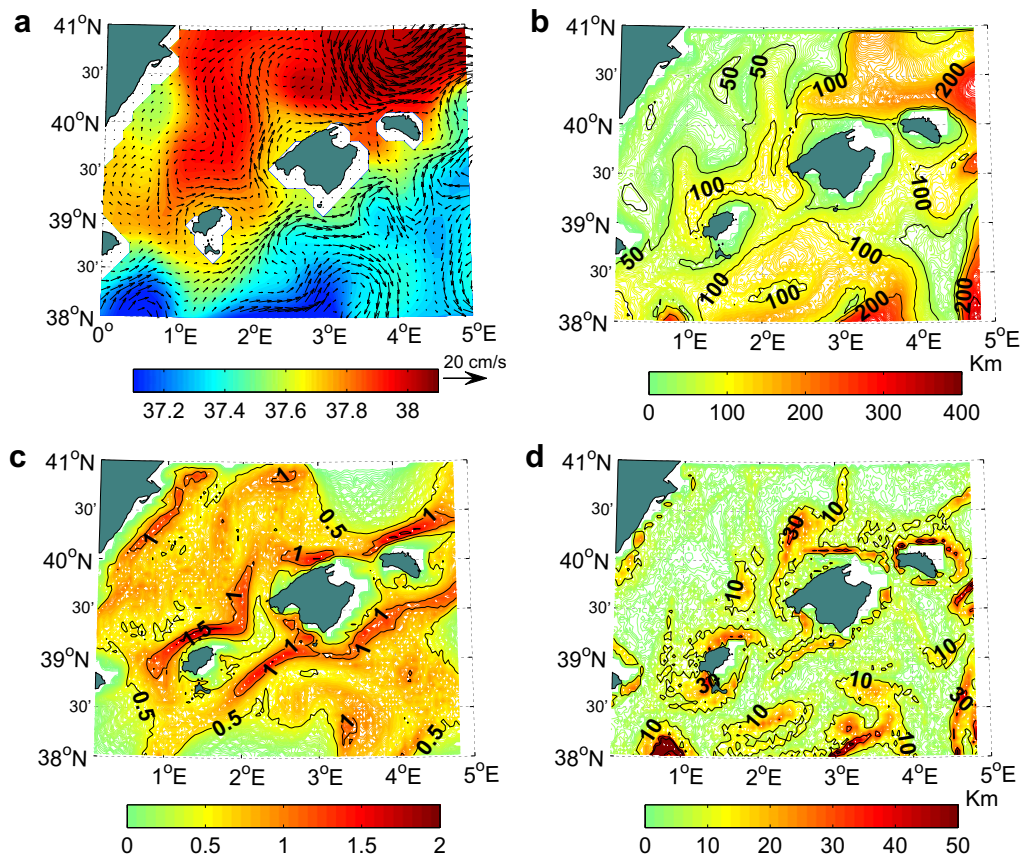


Fig. 6. Modelled ocean circulation and spatial patterns of bluefin tuna larvae in July 2003 in the Balearic area. (a) Velocity and salinity distribution at 35-m depth simulated for the 3rd of July 2003. (b) Averaged moved distances, (c) aggregation index and (d) dispersion of modelled bluefin tuna larvae.

with the results obtained in the aggregation pattern (Fig. 5c) that appears more homogeneous in the north.

Water masses in the southern section of our model domain were dominated by AW. The frontal region appears to be characterized by a narrow aggregation pattern lying south of Mallorca and Menorca, and a relatively strong aggregation west of Ibiza (Fig. 5c). This aggregation meander is surrounded by areas with much lower particle concentrations. In particular, a large gap is present around 2°30'E and 39°N, which is an area with relatively high dispersion properties and low velocities (Fig. 5a and d). Other areas of aggregations are present in the MW and especially in the coastal area influenced by the Balearic current.

These aggregation and dispersion patterns are consistent with the distributions of bluefin tuna larvae collected in the area and in the same period of 2001 (Garcia et al., 2003; see also Fig. 7a). Highest concentrations of bluefin tuna larvae were observed south of the islands and in the channels between the islands.

The distribution of tuna larvae in the Balearic area has also been analyzed for July 2003, when model results can be compared with observations. In July 2003, the circulation was characterized by a weak front south of the Balearic Islands (Fig. 6a) and therefore, much weaker mesoscale structures with respect to 2001. This results in a spatial distribution of modelled larvae that was very different from that estimated in 2001. In 2003, modelled larvae were aggregated along relatively narrow bands of water north of Ibiza and the Mallorca Channel, and south of the Mallorca Channel, Mallorca and Menorca (Fig. 6c). In comparison, modelled larvae in 2001 were most abundant in a wider strip of water farther south of the Mallorca Channel, Mallorca and Menorca (Fig. 5c).

Modelled larvae travelled shorter distances in 2003 (Fig. 6b) than modelled larvae did in June 2001 (Fig. 5b). For example, in a

large area south of Ibiza and Mallorca, eggs and larvae produced in 2001 travelled at least 200 km during the 20-day simulation (Fig. 5b), whereas they travelled ~100 km in 2003 (Fig. 6b). Larvae produced north of Ibiza and Mallorca in 2003 also moved shorter distances than in 2001.

The dispersion (Fig. 6d) also appears lower in 2003 although the highest values are still in the region of AW. The resulting spatial pattern of aggregation (Fig. 6c) was similar to that estimated for 2001 for the higher values (Fig. 5c) but with a much weaker spatial gradient. In general, all the patterns (distances travelled, aggregation, and dispersion) appear spatially more homogenous than those obtained in 2001.

In the aggregation maps (Figs. 5c and 6c), a few sites are characterized by very low values of the particle aggregation index (~0). These areas are the result of strong water advection from regions outside the analyzed domain where no particles were released. Hence, this flushing effect is particularly evident close to the coasts and close to the northern and southern boundaries of the numerical domain. However, the empty areas in the Menorca Channel in 2001 (Fig. 5c) and to a less extent in 2003 (Fig. 6c) were the result of a strong and rapid advection of water from below 35-m depth. This upwelling is likely connected to the Balearic Current flowing north of Mallorca and is also evident in our animations of the regional circulation (electronic Supplementary material; Videos 1 and 2).

3.3. Identification of probable spawning sites

We can reconstruct the probable spawning site of surviving eggs and larvae of bluefin tuna by extracting the initial position of those particles that at the end of the simulation were close to the observed positions of the larvae (Garcia et al., 2005b). The high-

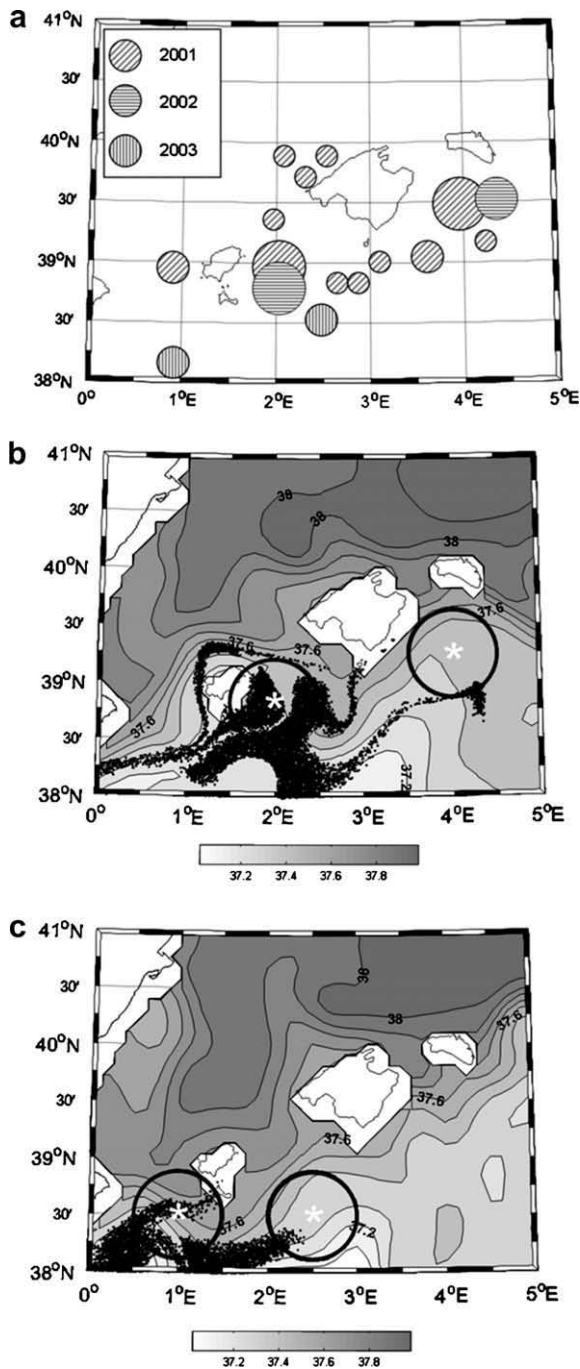


Fig. 7. (a) Reconstruction of the observed distribution of bluefin tuna larvae in 2001, 2002 and 2003 (after TUNIBAL project; Garcia et al., 2005b). Larger (smaller) circles represent higher (lower) probability of capture in the given area, and maps show the salinity distribution at 35-m depth and initial positions of the particles collected in the aggregation sites (circles) in (b) 2001 and in (c) 2003.

est field concentrations in 2001 were in the Mallorca Channel and west of Mallorca (Fig. 7a). According to the model, both areas (Fig. 7b, circles) are composed of particles that originated as eggs in a region south of Mallorca (Fig. 7b). Some of these eggs and larvae moved relatively large distances ($\langle d \rangle = 220$ km) with intermediate dispersion ($\langle \sigma \rangle \approx 13$ km) ending up in the Menorca Channel. Another group of particles aggregated in the Mallorca Channel but their drifting distance is shorter ($\langle d \rangle \approx 85$ km; $\langle \sigma \rangle \approx 15$ km) and their initial position is close to their spawning ground (Fig. 7b). A smaller group of particles appears to originate west of Ibiza along a pattern that resembles the coastal current of-

ten observed in that area. Considering both aggregation sites, the temperature experienced by larvae along the drift is 16.4–23.8 °C (average $T = 20.6$ °C) while the range of salinity is 37.0–37.5 psu (average $S = 37.3$ psu).

One of the most striking features of the spatial distribution of the origins of particles, which eventually overlapped with field-caught larvae, was that nearly all were located close to and along the Mediterranean–Atlantic front (salinity range 37.4–37.6 psu); this frontal region is evident from the modelled salinity distribution at 35-m depth (Fig. 7b) and is located west and north of Ibiza and the Mallorca Channel (see Fig. 8).

The distribution of larvae in the field in July 2003 appears much different from that in previous years. Larvae were located far from the coast and mainly south of Ibiza (Fig. 7a). By backtracking the particles collected in those areas at the end of the simulations, we can estimate the likely spawning sites in 2003 that produced these survivors (Fig. 7c). Most of the particles appeared to originate in an area close to their final position (southwest of Ibiza) indicating relatively little advection from the spawning site; this result is consistent with the modelled travelled distances in this year ($\langle d \rangle \approx 70$ km, $\langle \sigma \rangle \approx 10$ km; Fig. 6b).

However, as shown in the salinity distribution in 2003 (Fig. 7c) and consistent with the situation in 2001 (Fig. 7b), all particles were released close to the salinity front, whose position in 2003 was south of Ibiza (Fig. 7c and 8). The range in temperature experienced along the drift was 15.6–26.6 °C (average $T = 21.4$ °C) while the range of salinity was 36.8–37.7 psu (average $S = 37.2$ psu).

3.4. Seasonal and year-to-year variability in drift/retention patterns

The distribution of the salinity front (approximated as the position of the 37.5 psu isoline) around the Balearic Islands shows high year-to-year variability (Fig. 8). While in 1999 the front was ~ 100 km northwest of the Ibiza Island, it appeared to move southward and closer to the coast in 2000–2002. In 2003, the position appeared very different with the front lying ~ 80 km south of Ibiza. However, considering the average salinity distribution over different years and times of the year (June–July), the front appears to dwell on an east–west direction with stronger seasonal variability towards the eastern section (Fig. 8).

We can derive with a similar particle-tracking procedure as performed for 2001 and 2003 an average aggregation map for the years 1999–2003 (exp04). The map (Fig. 9a) shows a general aggregation area all around Mallorca with higher concentrations associated with the Balearic Current in the north, and close to the Mallorca and Menorca Channels in the south (Fig. 9a). However, this average aggregation map is highly variable both on year-to-year and seasonal scales.

Patchiness index, ψ , during 2003 was generally lower than in the other five years of our comparison (Fig. 9b). This was evident for nearly all months: ψ was much higher in June 2001–2002 than 2003. The low patchiness index in 2003 is consistent with the relatively homogeneous larval spatial distribution patterns discussed in the previous section. In some years, patchiness decreased throughout the summer whereas in other summers, it was similar in all months (1999, 2003) or even slightly increased (2000).

3.5. Correlation between patchiness index and general circulation of the NW Mediterranean

The NW Mediterranean Sea has a generally cyclonic circulation connecting the Ligurian Sea, Gulf of Lions and Balearic Sea, and whose strength is related to the baroclinic and barotropic responses to wind forcing.

It can then be of interest to investigate whether there is a qualitative correlation at interannual scales between the local

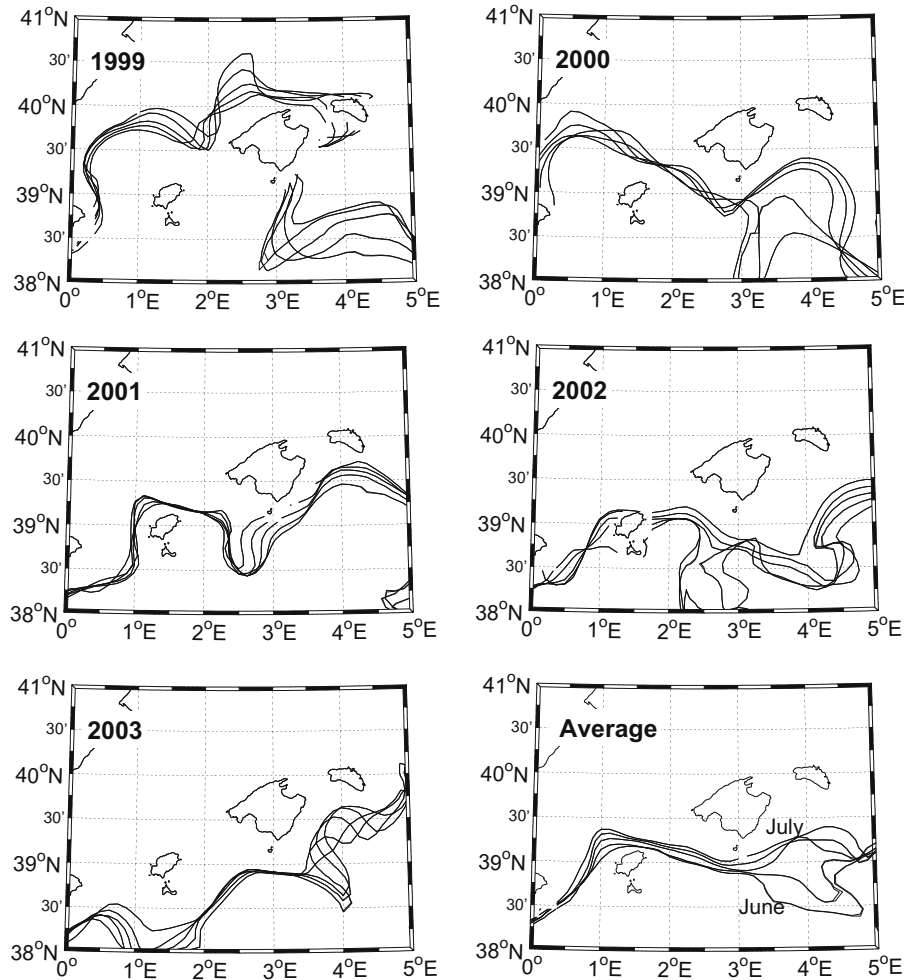


Fig. 8. Positions of the 37.5 psu contour at 35-m depth in the Balearic area. Data are shown for the years 1999–2003 and for the five emissions simulated in June and July (*exp04*, Table 1). The average (over years) front position for each of the five emission periods considered in the simulations (every ten days in June–July) are also shown.

patchiness index (ψ , Eq. (3)) and the atmospheric forcing of the NW Mediterranean that was used in the model (ECMWF analysis; Fig. 10). We, therefore, conducted an exploratory analysis to evaluate the hypothesis that interannual variability in the year-specific averaged patchiness in the Balearic area covaried with the mean June–July values of the wind stress (Fig. 10a), the wind zonal component (Fig. 10b) and the air temperature (Fig. 10c) at two locations (Gulf of Lyons, 42°N, 5°E; Balearic Islands, 48°N, 2°E; Fig. 1). We also used the difference between the zonal wind stress in the Gulf of Lyons and a southern location whose latitude corresponded to that of the Balearic Islands (48°N, 5°E) as proxy for the large-scale wind stress curl in the NW Mediterranean. We then compared this proxy with the average patchiness index (Fig. 10d).

Results show that patchiness tended to be higher when both the wind stress (Fig. 10a), the zonal component of the wind (Fig. 10b) and the derived wind curl (Fig. 10d) were larger, while a strong decrease of ψ occurred when air temperature increased (Fig. 10c). These relations are more evident when the atmospheric forcing in the Gulf of Lyons (squares) was considered.

4. Discussion

4.1. General patterns

We have developed and applied an initial version of a process-based model of the ecology of early life-history stages for anchovy

and bluefin tuna in the Mediterranean Sea. For both species, the simulated drift of eggs and larvae are fairly similar to the observed larvae distributions. These similarities suggest that the model and its assumptions are capable of reproducing many of the key processes and features of both the biology of the species and the local hydrography.

Along the Catalan coast, the model produces a weaker salinity gradient compared to that observed in June 2000 (Sabates et al., 2007b). This results in a weaker flow at the shelf boundary which impacts the southward transport of tracers and anchovy larvae along the shelf-break yielding a significant difference between predicted particles' drift and the observed drogues positions (Fig. 4). However, it should also be noted that at day 5 of the Lagrangian experiment in Sabates et al. (2007b), an intense storm crossed the area forcing the interruption of the survey for 30 h. While the modelled circulation was affected by this event, the detailed effects of the storm on particle dispersion might not be accurately represented since atmospheric forcing is applied on a daily average and the oceanographic dataset has a 5-day resolution. We recognize that although the model is eddy-permitting, it cannot entirely reproduce observed wind-driven mesoscale activity without data assimilation.

Most of the circulation patterns observed in the Balearic area were well represented in our circulation model. The strong Balearic Current is always present in the summer months close to the coastal area of the Balearic Islands. The current in 2001 was part of a local advection of water from deeper layers (<35 m) in an area

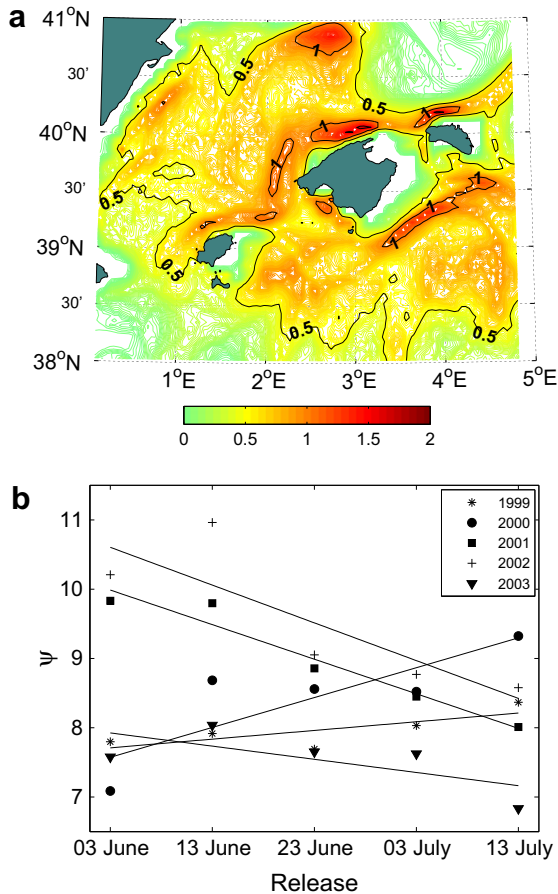


Fig. 9. (a) Map of the aggregation index of bluefin tuna larvae obtained as an average over five years (1999–2003) and over the six particle releases in the period June–July (*exp04*). (b) Patchiness index as function of the spawning period for the years 1999–2003.

close to the Menorca Channel. Several mesoscale structures were present in our simulations and they are mainly driven by interactions among waters of Atlantic and Mediterranean origins, plus the interaction with topography. The anticyclonic circulation around Ibiza is also well reproduced and in 2001, this structure contributes to the dispersion and aggregation patterns along the thermohaline front.

Spatial distributions of the modelled bluefin tuna larvae and salinity can be characterized as being dominated by mesoscale (10s–100s km) patchiness and variability. Several gyre-like and frontal features are evident in both the larval and hydrographic distributions. These features have been reported earlier using satellite imagery and direct sampling (Garcia et al., 2003; Alemany et al., 2006; Sabates et al., 2007a). Several mechanisms are responsible for this hydrographic variability (Sabates et al., 2007a) and include: the inflow of Atlantic water, the residual circulation of the wider Mediterranean Sea, and interaction of these flows with land-masses, including the Balearic Islands (Bakun, 2006; Garcia et al., 2006b), regional wind conditions, and river runoff (Agostini and Bakun, 2002). These processes can potentially establish local areas with enhanced plankton production (Agostini and Bakun, 2002; Bakun, 2006). How and whether fish larvae benefit from these structures can in future be investigated by using the modelling approaches developed here, in combination with ecosystem models of plankton production.

The biological component of our model is relatively simple when compared to existing biological–physical oceanographic

models of larval fish ecology (Hinckley et al., 1996; Werner et al., 2001; Hinrichsen et al., 2003b). We presently have a poor-knowledge of bluefin tuna larval ecology (e.g. vertical migratory behaviour, temperature and food-dependence of growth and survival rates, and larval dietary preferences), and we had to use pragmatic descriptions and assumptions of some key rates and behaviours of bluefin tuna larvae. Our description of growth is representative of the length-at-age distribution of surviving bluefin tuna larvae observed in the Balearic area (Garcia et al., 2003, 2006a), but the sensitivity of our model outputs to biological assumptions deserves further investigation. In particular, the vertical distribution and buoyancy of eggs and larvae needs more study. Many species of larvae typically develop vertical migratory behaviour during ontogeny. Moreover, if larval food is located below the upper 35 m where our simulated larvae resided, they may perform vertical migrations to deeper layers where copepod nauplii aggregate (Sabates et al., 2007a). Such vertical migrations, if performed by bluefin tuna larvae, could influence their horizontal displacement and our interpretations of transport and retention.

Knowledge gaps, such as those noted above, can potentially be filled in the future so that outputs can be improved. However, under the assumptions and limits of our approach, the correspondence between our modelled larval distributions and those observed in the field (Garcia et al., 2005b) for different years, having very different hydrographic forcing, suggest that the approach is capable of representing many of the main features of larval growth and drift. Comparisons with different species and years suggests that our modelling approach can be used to simulate drift and growth of bluefin tuna and anchovy eggs and larvae in the Mediterranean Sea, and for assessing the importance of productivity triads (Agostini and Bakun, 2002; Bakun, 2006). Moreover, tuna larvae become piscivorous and cannibalistic at a relatively small size (5–6 mm; Young and Davis, 1990; Catalan et al., 2007), as do other scombrid larvae (Hillgruber and Kloppmann, 2001). We believe that the model developed here could potentially be used in a multi-species context to investigate the potential for bluefin tuna predation on other species (e.g. anchovy) and itself (cannibalism). For example, by releasing modelled larvae at different times of the year and mapping the spatial overlap of the early-spawned and late-spawned survivors within a spawning season, the potential for cannibalism in the field could be identified.

4.2. Spatial patterns

Model results suggest that mesoscale processes affecting exchanges between different water masses (i.e. MW and AW) are regulating spawning of bluefin tuna in the Balearic area. Eggs are released in proximity of the front and in Atlantic waters, while larvae are dispersed by local circulation that is influenced by the shape of the baroclinic meanders (Fig. 11). These structures commonly produce convergent and divergent structures characterized by local vertical velocities that can be one order of magnitude higher than the largest vertical velocity usually observed in upwelling areas (Tintore et al., 1991; Pinot et al., 1995; Velez-Belchi and Tintore, 2001). In the summer of 2001, our model simulations showed an intense upwelling of water from 35-m depth in proximity of the Menorca Channel, very close to one of the aggregation sites for bluefin tuna larvae (Fig. 11).

In summary, the Balearic area in the period of bluefin tuna spawning appears mainly affected by the ocean front that promotes an atypical “ocean triad” where aggregation patterns and retention sites produced by mesoscale processes with strong vertical dynamics (upwelling) are located close to each other (Fig. 11) and not spatially segregated (Agostini and Bakun, 2002). This combination of mesoscale processes yields favorable reproductive habitat during the period of larval development (Sabates et al., 2007a).

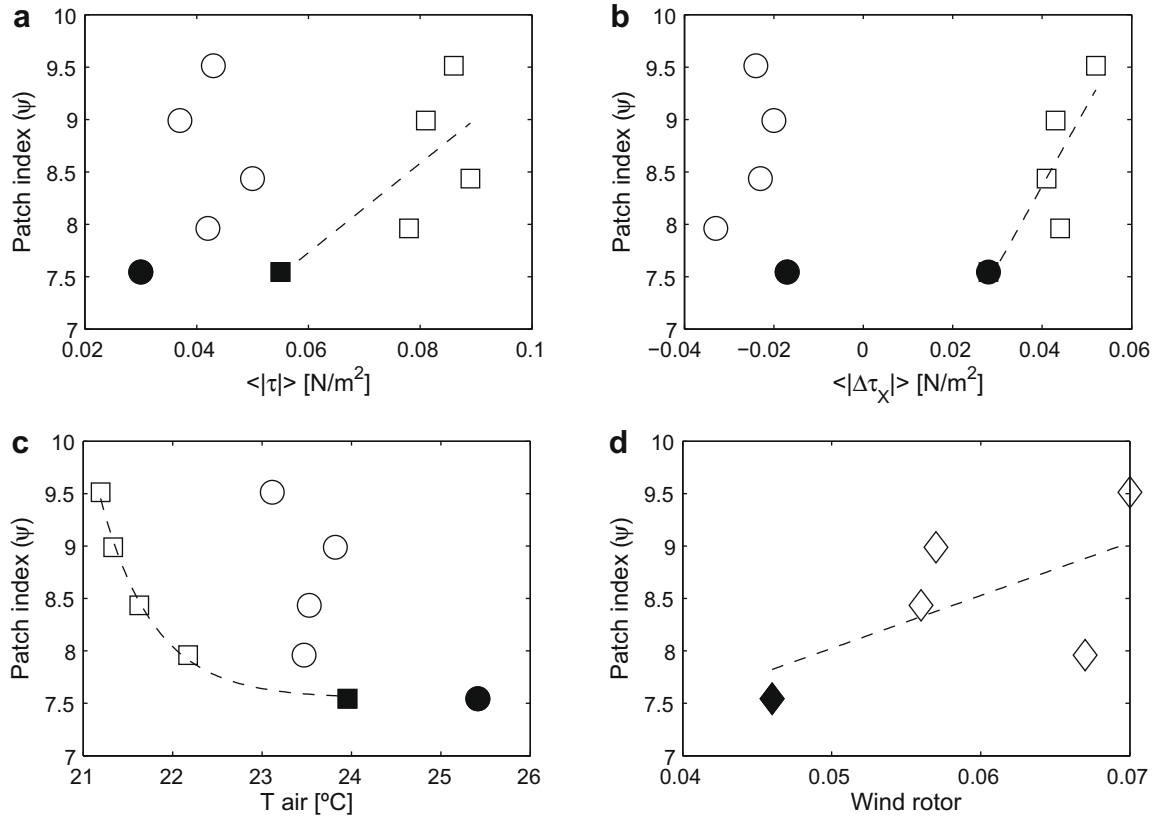


Fig. 10. Relationships between the average patchiness index (ψ) and averaged meteorological variables measured at two locations (Gulf of Lyons, 42°N, 5°E, squares; Balearic Islands, 48°N, 2°E, circles) for: (a) wind stress, $|\tau|$, (b) zonal component of the wind, τ_x , (c) air temperature, (d) curl of the wind in the NW Mediterranean (difference in τ_x , between 42°N and 48°N at 5°E). Open symbols used for the years 1999–2002 while solid symbols used for 2003. In plotting the lines, a linear fitting was applied in (a), (b) and (d) while in (c) an exponential fitting of the form $y = ae^{bx} + c$ was used.

We observed different patterns of spatial variability in the modelled distributions in 2001 and 2003. These differences were also reported from field data (Garcia et al., 2005b) and we suggest that they are related to the positions of the Balearic front (Fig. 8). The generally higher stratification associated with intense summer heating and lower wind speeds in 2003 (e.g. Olita et al., 2007) produces a thermohaline structure and circulation patterns much different from those in 2001. In 2003, the Mediterranean suffered the impact of an unusual atmospheric heatwave related to an increase of air temperature, decrease in wind stress and reduction of other atmospheric fluxes (Black et al., 2004; Schar et al., 2004; Olita et al., 2007). This anomalous heating influenced the thermal structure of the upper 15 m of the Mediterranean Sea resulting in a stronger stratification and reduced mixing (Sparnocchia et al., 2006; Olita et al., 2007) 2003 was the warmest year in Europe during the last 500 years (Luterbacher et al., 2004). The ability of our model to reproduce the larval distribution in such an exceptional year suggests that it may be useful for investigating a wide range of climatic scenarios, including those expected under future climate change. Interestingly, the spawning area identified in 2001 by our modelling exercise (schematically represented in Fig. 11), not only corresponds to the site where small larvae were captured (Garcia et al., 2005b), but also to the area where electronically tagged bluefin tunas swam during June 2001 and June–July 2003 (Block et al., 2003, 2005), and more generally to the spatial distribution of commercial fishing vessels targeting bluefin tuna (Garcia et al., 2005b; Fig. 11).

The patchiness index (ψ , Eq. (3)) around the Balearic Islands is related to local ocean dynamics and in particular to the position and intensity of the local fronts and associated mesoscale eddy

field, which are in turn related to the atmospheric forcing and bottom topography. In this particular area, no specific studies have yet investigated the relation between the position and strength of the frontal region south of the Balearic Islands and the atmospheric forcings. The region is a transition between the NW Mediterranean circulation and the circulation in the Algerian basin, characterized by the fresher AW. The NW Mediterranean has a generally cyclonic circulation forced by local wind regimes, e.g. Tramontana and Mistral wind, whose effects on the ocean are mainly in the Gulf of Lyons (Heburn, 1987).

As a consequence, the correlations between our estimates of ψ and the local atmospheric forcings (Fig. 10) showed a clearer relation when data in the Gulf of Lyons were considered. We argue that this difference in spatial forcing of patchiness near the Balearic Islands probably reflects the major influence of winds blowing over the Gulf of Lyons in the large-scale circulation of the NW Mediterranean Sea, because of topographic and planetary- β effects (Hogg, 1973; Madec et al., 1996; Herbaut et al., 1997). However, probably the most ecologically relevant result is that the patchiness seemed to decay exponentially with increases in the air temperature in the Gulf of Lyons (Fig. 10c) which, in summer and in the Mediterranean region, are generally related to the local heat balance more than to remote advective contributions, e.g. the sensible heat flux component has its minimum in July–August (Ruiz et al., 2008).

The presence of the atmospheric heatwave over Europe in the summer of the 2003 appears to have strongly reduced the mesoscale activity in the model and hence led to an exponential reduction of ψ . Since these anomalous atmospheric conditions are expected to become more frequent as climate change progresses in the 21st century (IPCC, 2007), bluefin tuna larvae could experi-

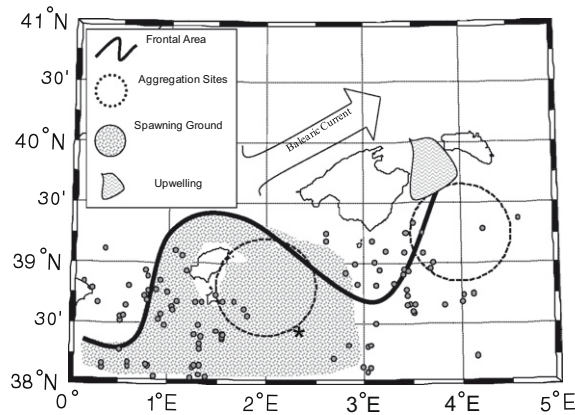


Fig. 11. Schematic representation of the physical and biological processes involved in the spawning location and larval distribution of bluefin tuna in 2001 in the Balearic area. The shape of the front and the associated mesoscale activity controls the position of the spawning ground and the locations of the aggregations and enrichment sites. Gray dots (●) are the positions of purse-seine tuna fishing fleet spotted by aerial sightings from June 28 to July 29, 2001 (Garcia et al., 2003) while the black star (★) is the recapture position of a tagged bluefin tuna on June 3rd, 2001 (Block et al., 2003).

ence a reduction of mesoscale oceanographic activity in the Balearic area. The resulting hydrodynamics conditions will then be different from those to which bluefin tuna has adapted its spawning behaviour in the NW Mediterranean.

4.3. Modelling aspects and limitations

The movement of the numerical particles was simulated using a Lagrangian individual-based model that includes a deterministic term (related to the fluid velocity), a stochastic term (accounting for the mixing processes) and a biological term (larvae swimming velocity). All those components interact to determine the particles' individual displacement, although their magnitudes differed.

The deterministic component has the largest influence in the 20 days drifting period especially in the Balearic area where velocities can easily exceed 20 cm/s (Figs. 5 and 6). In comparison, the biological term related to larval swimming velocity, and hence the assumed growth model, is relatively minor. The total displacement in 20 days due to the swimming is in any case at least an order of magnitude lower than that produced by the fluid velocity. Nevertheless, this term was included in our particle-tracking algorithm because it produces a more general description of the larval vertical positions and thus a more robust simulation of the dispersion processes. However, our description of growth is only a first approximation and deserves further investigation. We suggest that a more rigorous estimation can be obtained using a growth-temperature model that combines daily otolith increments of bluefin tuna larvae in the Balearic with the modelled temperature experienced by larvae while drifting (Mariani et al., 2008).

The displacement derived from the stochastic term is time-step dependent: the shorter the time step is, the larger the total displacement of the particles. Therefore, the absolute values reported in the moved distance and dispersion maps, can only provide the order of magnitude of these parameters rather than exact quantities. However, to account for such effects we performed simulations similar to *exp03* but with the random displacement model switched off. We then re-evaluated the spatial maps (Figs. 5 and 6) obtaining almost the same patterns but with ~10% difference in the moved distances.

Consequently, although it is simpler and might be reasonable to model only the deterministic term of the tracking model (Lett et al.,

2006, 2007), we think that the stochastic component and a large number of numerical particles allowed the model to provide a more robust statistic of the turbulence dispersion patterns in the Balearic area. Moreover, the addition of size-dependent swimming behaviour could also shape the spatial patterns in different years or different times of the year, particularly if non-random swimming directions were included. However, the evaluation of the relative importance of each term in producing the observed spatial pattern needs further investigation.

Our definitions of retention and dispersion processes are different from those used by other authors in upwelling areas (Lett et al., 2006, 2007). We estimated retention as the combination of two different processes: the averaged distance moved by a group of particles and its variance (Hinrichsen et al., 2003b). We did not directly quantify the enrichment (Lett et al., 2006, 2007) but areas of enrichment can be identified from locations of low values of aggregation and from the dynamics of the particles dispersion (Videos 1 and 2 in the Supplementary Electronic material). It is also worth noting that aggregations of passive particles is possible in our model since eggs and larvae were constrained in the first 35 m and therefore they can easily aggregate in converging areas (such as fronts) with mechanisms that realistically reproduce observed behaviour of planktonic organisms (Genin et al., 2005).

4.4. Contribution to fisheries management

The abundance of bluefin tuna has declined significantly since the 1970s and a new management plan for the recovery of the population in the eastern Atlantic–Mediterranean has recently been implemented (ICCAT, 2008a). There are also problems with unreported and misreported commercial catches of bluefin tuna in the Mediterranean (ICCAT, 2008b). The fisheries have become increasingly regulated in recent years, including the establishment of quotas in the east Atlantic–Mediterranean in the late 1990s, and an increase in minimum landing size in the Mediterranean in 2007 to reduce captures of juvenile tuna (ICCAT, 2008b).

Improvements in understanding the reproductive biology and processes affecting early life history could contribute to the management of tuna populations in several ways. First the identification of spawning areas, combined with hydrographic model estimates of retention/loss of spawning products, could be the basis for developing fishery-independent recruitment indices.

Second, the identification of spawning areas and the quantification of their utilization could be a step toward the development of marine protected areas or areas closed to fishing of bluefin tuna or other species of interest. Establishment of such areas to promote recovery of bluefin tuna could potentially be beneficial, but the locations, sizes, shapes, and timing (seasonal and multi-annual duration) of such areas, and their implementation in relation to other regulations, needs to be considered carefully to provide the most benefit. In particular, knowledge of where spawning and nursery sites are located and how these locations vary with population characteristics (abundance, age/size structure) and hydrographic forcing is needed.

Some of this knowledge can be acquired directly through fieldwork of distributions of larval, juvenile and spawning adults (e.g. Karakulak et al., 2004; Garcia et al., 2005a; Teo et al., 2007), particularly when combined with process-based modelling studies. For example, our results, and those of Garcia (Garcia et al., 2003, 2005a, 2005b; 2006), suggest that it may be possible to identify the most likely spawning areas based on knowledge of water mass characteristics (e. g. temperature, salinity, density), and the most likely sites of 0-group nursery areas under different hydrographic conditions, as has been shown for fish larvae in other ecosystems (Hinrichsen et al., 2003a; Brickman et al., 2007).

Third, modelling approaches such as those developed here can also be used to reconstruct the locations of spawning areas of juveniles recovered in different areas (Christensen et al., 2007). This information could be helpful in quantifying the spatial contributions of different spawning areas (e. g. Balearic area, Sicily, Cyprus) to juvenile production, how these contributions change over time, and the potential for mixing of offspring from different areas. Applications of this modelling approach to topics such as these could improve the ecosystem basis for management of this stock.

Acknowledgements

This work is a contribution to a European Network of Excellence on Ocean Ecosystems Analysis (www.eur-oceans.org) and GLOBEC. PM was supported by a EUR-OCEANS postdoctoral fellow grant and by the Technical University of Denmark (DTU-Aqua; formerly Danish Institute for Fisheries Research) and the Stazione Zoologica “Anton Dohrn” (Napoli, Italy). We thank Dr. F. Köster and Dr. M. Ribera d’Alcalá for assistance and Drs. A. Christensen, A. Riccio, A. Visser, H.H. Hinrichsen and U.H. Thygesen for discussions regarding particle drifting algorithm.

Appendix A. Supplementary data

Supplementary data associated with this article can be found, in the online version, at [doi:10.1016/j.pocean.2010.04.027](https://doi.org/10.1016/j.pocean.2010.04.027).

References

- Agostini, V.N., Bakun, A., 2002. “Ocean triads” in the Mediterranean Sea: physical mechanisms potentially structuring reproductive habitat suitability (example application to European anchovy, *Engraulis encrasicolus*). *Fisheries Oceanography* 11, 129–142.
- Alemany, F., Deudero, S., Morales-Nin, B., Lopez-Jurado, J.L., Jansa, J., Palmer, M., Palomera, I., 2006. Influence of physical environmental factors on the composition and horizontal distribution of summer larval fish assemblages off Mallorca Island (Balearic archipelago, western Mediterranean). *Journal of Plankton Research* 28, 473–487.
- Alhammoud, B., Beranger, K., Mortier, L., Crepon, M., Dekeyser, I., 2005. Surface circulation of the Levantine Basin: comparison of models results with observations. *Progress in Oceanography* 66, 299–320.
- Astraldi, M., Gasparini, G.P., 1992. The seasonal characteristics of the circulation in the North Mediterranean Basin and their relationship with the atmospheric-climatic conditions. *Journal of Geophysical Research* 97, 9531–9540.
- Astraldi, M., Gasparini, G.P., Vetrano, A., Vignudelli, S., 2002. Hydrographic characteristics and interannual variability of water masses in the central Mediterranean: a sensitivity test for long-term changes in the Mediterranean Sea. *Deep-Sea Research I* 49, 661–680.
- Bakun, A., 2006. Fronts and eddies as key structures in the habitat of marine fish larvae: opportunity, adaptive response and competitive advantage. *Scientia Marina* 70, 105–122.
- Black, E., Blackburn, M., Harrison, G., Hoskin, B., Methven, J., 2004. Factors contributing to the summer 2003 European heatwave. *Weather* 59, 217–222.
- Blanke, B., Delecluse, P., 1993. Variability of the tropical Atlantic Ocean simulated by a general circulation model with two different mixed-layer physics. *Journal of Physical Oceanography* 23, 1363–1388.
- Block, B.A., Boustany, A., Teo, S.L.H., Walli, A., Farwell, C.J., Williams, T.D., Prince, E.D., Stokesbury, M.J.W., Dewar, H., Seitz, A.C., Weng, K.C., 2003. Distribution of western tagged Atlantic bluefin tuna determined from archival and pop-up satellite tags. *ICCAT Collective Volume of Scientific Papers* 55, 1127–1139.
- Block, B.A., Teo, S.L.H., Walli, A., Boustany, A., Stokesbury, M.J.W., Farwell, C.J., Weng, K.C., Dewar, H., Williams, T.D., 2005. Electronic tagging and population structure of Atlantic bluefin tuna. *Nature* 434, 1121–1127.
- Bozec, A., Bouruet-Aubertot, P., Beranger, K., Crépon, M., 2006. Mediterranean oceanic response to the interannual variability of a high-resolution atmospheric forcing: a focus on the Aegean Sea. *Journal of Geophysical Research* 111, C11013. doi:10.1029/2005JC003427.
- Bozec, A., Bouruet-Aubertot, P., Judicone, D., Crépon, M., 2008. Impact of penetrative solar radiation on the diagnosis of water mass transformation in the Mediterranean Sea. *Journal of Geophysical Research* 113, C06012. doi:10.1029/2007JC004606.
- Brickman, D., Marteinsdottir, G., Logeman, K., Harms, I.H., 2007. Drift probabilities for Icelandic cod larvae. *ICES Journal of Marine Science* 64, 49–59.
- Catalan, I.A., Alemany, F., Morillas, A., Morales-Nin, B., 2007. Diet of larval albacore *Thunnus alalunga* (Bonnaterre, 1788) off Mallorca Island (NW Mediterranean). *Scientia Marina* 71, 347–354.
- Christensen, A., Daewel, U., Jensen, H., Mosegaard, H., St John, M., Schrum, C., 2007. Hydrodynamic backtracking of fish larvae by individual-based modelling. *Marine Ecology Progress Series* 347, 221–232.
- Cury, P., Anneville, O., Bard, F.X., Fonteneau A., Roy, C., 1998. Obstinate north Atlantic bluefin tuna (*Thunnus thynnus thynnus*): an evolutionary perspective to consider spawning migration, ICCAT collective volume of scientific papers. In: *Proceedings of ICCAT Tuna Symposium 1998*. Part 1, vol. 62, pp. 239–247.
- de Boor, C., 1978. *A Practical Guide to Splines*. Springer-Verlag, New York.
- Fromentin, J.-M., Powers, J.E., 2005. Atlantic bluefin tuna: population dynamics, ecology, fisheries and management. *Fish and Fisheries* 6, 281–306.
- García, A., Alemany, F., Velez-Belchi, P., Lopez-Jurado, J.L., de la Serna, J.M., Gonzales Pola, C., Rodriguez, J.M., Jansa, J., 2003. Bluefin tuna and associated species spawning grounds in the oceanographic scenario of the Balearic Archipelago during June 2001. *ICCAT Collective Volume of Scientific Papers* 55, 138–148.
- García, A., Alemany, F., de la Serna, J.M., Oray, I., Karakulak, S., Rollandi, L., Arigò, A., Mazzola, S., 2005a. Preliminary results of the 2004 bluefin tuna larval surveys off different Mediterranean sites (Balearic Archipelago, Levantine Sea and the Sicilian Channel). *ICCAT Collective Volume of Scientific Papers* 58, 1420–1428.
- García, A., Alemany, F., Velez-Belchi, P., Lopez-Jurado, J.L., Cortes, D., de la Serna, J.M., Gonzales Pola, C., Rodriguez, J.M., Jansa, J., 2005b. Characterization of bluefin tuna spawning habitat off the Balearic Archipelago in relation to key hydrographic features and associated environmental conditions. *ICCAT Collective Volume of Scientific Papers* 58, 535–549.
- García, A., Cortes, D., Ramirez, T., Fehri-Bedoui, R., Alemany, F., Rodriguez, J.M., Carpena, A., Alvarez, J.P., 2006. First data on growth and nucleic acid and protein content of field-captured Mediterranean bluefin (*Thunnus thynnus*) and albacore (*Thunnus alalunga*) tuna larvae: a comparative study. *Scientia Marina* 70, 67–78.
- García, S., Boucher, J., Cury, P., Thébaud, O., Andriantsoa, M., Astudillo, A., Ba, M., Brander, K., Charles, A., Dulvy, N., Gauthiez, F., Heip, C., Jennings, S., Joannot, P., McDonald, D., MacKenzie, B., Rice, J., <<http://www.ifremer.fr/com/muniques/28-01-05-ifremer-biodiversite-restitution-atelier.htm>>, 2006b. Workshop 10, Paris Conference: Biodiversity, Science and Governance, Jan. 24–28, 2005 (Report of the Debates and Proposed Priority Actions. Ministry of Foreign Affairs, Government of France, Paris: 1–2).
- Genin, A., Jaffe, S.J., Reef, R., Richter, C., Franks, P.J.S., 2005. Swimming against the flow: a mechanism of zooplankton aggregation. *Science* 308, 860–862.
- Heburn, G.W., 1987. The dynamics of the western Mediterranean Sea: a wind forced case study. *Annales Geophysicae B* 5, 61–74.
- Herbaut, C., Martel, F., Crepon, M., 1997. A sensitivity study of the general circulation of the Western Mediterranean Sea. Part II: the response to atmospheric forcing. *Journal of Physical Oceanography* 27, 2126–2145.
- Hillgruber, N., Kloppmann, M., 2001. Small-scale patterns in distribution and feeding of Atlantic mackerel (*Scomber scombrus* L.) larvae in the Celtic Sea with special regard to intra-cohort cannibalism. *Helgolander Marine Research* 55, 135–149.
- Hinckley, S., Hermann, A.J., Megrey, B.A., 1996. Development of a spatially explicit, individual-based model of marine fish early life history. *Marine Ecology Progress Series* 139, 47–68.
- Hinrichsen, H.H., Bottcher, U., Koster, F.W., Lehmann, A., St John, M.A., 2003a. Modelling the influences of atmospheric forcing conditions on Baltic cod early life stages: distribution and drift. *Journal of Sea Research* 4, 187–201.
- Hinrichsen, H.H., Lehmann, A., Mollmann, C., Schmidt, J.O., 2003b. Dependency of larval fish survival on retention/dispersion in food limited environments: the Baltic Sea as a case study. *Fisheries Oceanography* 12, 425–433.
- Hogg, N., 1973. The preconditioning phase of MEDOC 1969, II, Topographic effects. *Deep-Sea Research* 20, 449–459.
- Houde, E.D., 1989. Comparative growth, mortality and energetics of marine fish larvae: temperature and implied latitudinal effects. *Fisheries Bulletin* 87, 471–496.
- ICCAT, 2008a. Recommendation Amending the Recommendation by ICCAT to Establish a Multi-annual Recovery Plan for Bluefin Tuna in the Eastern Atlantic and Mediterranean, pp. 1–27.
- ICCAT, 2008b. Report for the Biennial Period, 2006–2007. Part II. ICCAT, Madrid, Spain, pp. 1–266.
- CC, I.P., 2007. Summary of policymakers. In: Solomon, S., Qin, D., Manning, M., Chen, Z., Marquis, M. (Eds.), *Climate Change 2007: The Fourth Assessment Report*. Cambridge University Press, Cambridge, UK, pp. 1–18.
- Karakulak, S., Oray, I., Corriero, A., Deflorio, M., Santamaria, N., Desantis, A., De Metrio, G., 2004. Evidence of a spawning area for the bluefin tuna (*Thunnus thynnus* L.) in the eastern Mediterranean. *Journal of Applied Ichthyology* 20, 318–320.
- Kawamura, G., Masuma, S., Tezuka, N., Koiso, M., Jinbo, T., Namba, K., 2003. Morphogenesis of sense organs in the bluefin tuna *Thunnus orientalis*. In: Browman, H.I., Skiftesvik, A.B. (Eds.), *The Big Fish Bang*. Proceedings of the 26th Annual Larval Fish Conference. Institute of Marine Research, Bergen, Norway, pp. 123–135.
- Let, C., Roy, C., Levasseur, A., Van der Lingen, C.D., Mullon, C., 2006. Simulation and quantification of enrichment and retention processes in the southern Benguela upwelling ecosystem. *Fisheries Oceanography* 15, 363–372.
- Let, C., Penven, P., Ayón, P., Fréon, P., 2007. Enrichment, concentration and retention processes in relation to anchovy (*Engraulis ringens*) eggs and larvae distributions in the northern Humboldt upwelling ecosystem. *Journal of Marine Systems* 64, 189–200.

- Luterbacher, J., Dietrich, D., Xoplaki, E., Grosjean, M., Wanner, H., 2004. European seasonal and annual temperature variability, trends and extremes since 1500. *Science* 303, 1499–1503.
- Mackenzie, B.R., Leggett, W.C., Peters, R.H., 1990. Estimating larval fish ingestion rates: can laboratory derived values be reliably extrapolated to the wild? *Marine Ecology Progress Series* 67, 209–225.
- Madec, G., Lott, F., Delecluse, P., Crepon, M., 1996. Large-scale preconditioning of deep-water formation in the Northwestern Mediterranean Sea. *Journal of Physical Oceanography* 26, 1393–1408.
- Madec, G., Delecluse, P., Imbard, M., Lévy, C., 1998. OPA 8.1 Ocean General Circulation Model Reference Manual. Institute Pierre-Simon Laplace, pp. 1–91.
- Mariani, P., Garcia, A., MacKenzie, B., Alemany, F., Cortes, D., Velez-Belchi, P., 2008. Hindcasting the temperature and growth history of surviving larvae of bluefin tuna (*Thunnus thynnus*) in the NW Mediterranean Sea. In: Proceeding of the 32nd Annual Larval Fish Conference.
- Mather, F.J., Mason, J.M., Jones, A.C., 1995. Historical Document: Life History and Fisheries of Atlantic Bluefin Tuna. US Department of Commerce, NOAA, NMFS, Southeast Fisheries Science Center, pp. 1–165.
- MEDOC Group, 1970. Observation of formation of deep water in the Mediterranean Sea. *Nature* 227, 1037–1040.
- Millot, C., 1999. Circulation in the Western Mediterranean Sea. *Journal of Marine Systems* 20, 423–442.
- Miyashita, S., Sawada, Y., Okada, T., Murata, O., Kumai, H., 2001. Morphological development and growth of laboratory-reared larval and juvenile *Thunnus thynnus* (Pisces: Scombridae). *Fisheries Bulletin* 99, 601–616.
- North, E.W., Hood, R.R., Chao, S.Y., Sanford, L.P., 2006. Using a random displacement model to simulate particle motion in a baroclinic frontal zone: a new implementation scheme and model performance tests. *Journal of Marine Systems* 60, 365–380.
- Olita, A., Sorgente, R., Natale, S., Gabersek, S., Ribotti, A., Bonanno, A., Patti, B., 2007. Effects of the 2003 European heatwave on the Central Mediterranean Sea: surface fluxes and the dynamical response. *Ocean Science* 3, 273–289.
- Pacanowski, R.C., Gnanadesikan, A., 1998. Transient response in a z-level ocean model that resolves topography with partial cells. *Monthly Weather Review* 126, 3248–3270.
- Palomera, I., Olivar, M.P., Salat, J., Sabates, A., Coll, M., Garcia, A., Morales-Nin, B., 2007. Small pelagic fish in the NW Mediterranean Sea: an ecological review. *Progress in Oceanography* 74, 377–396.
- Pinot, J.M., Tintore, J., LopezJurado, J.L., Fernandez De Puelles, M.L., Jansa, J., 1995. Three-dimensional circulation of a mesoscale eddy/front system and its biological implications. *Oceanologica Acta* 18, 389–399.
- Pinot, J.M., Lopez-Jurado, J.L., Riera, M., 2002. The CANALES experiment (1996–1998). Interannual, seasonal, and mesoscale variability of the circulation in the Balearic Channels. *Progress in Oceanography* 55, 335–370.
- Robinson, A.R., Sellschopp, J., Warn-Varnas, A., Leslie, W.G., Lozano, C.J., Haley Jr., P.J., Anderson, L.A., Lermusiaux, P.F.J., 1999. The Atlantic Ionian Stream. *Journal of Marine Systems* 20, 129–156.
- Ross, O.N., Sharples, J., 2004. Recipe for 1-D Lagrangian particle tracking models in space-varying diffusivity. *Limnology and Oceanography: Methods* 2, 289–302.
- Ruiz, S., Gomis, D., Sotillo, M.G., Josey, S.A., 2008. Characterization of surface heat fluxes in the Mediterranean sea from 44-year high-resolution atmospheric data set. *Global and Planetary Change* 63, 258–274.
- Sabates, A., Olivar, M.P., Salat, J., Palomera, I., Alemany, F., 2007a. Physical and biological processes controlling the distribution of fish larvae in the NW Mediterranean. *Progress in Oceanography* 74, 335–376.
- Sabates, A., Salat, J., Palomera, I., Emelianov, M., Fernandez De Puelles, M.L., Olivar, M.P., 2007b. Advection of anchovy (*Engraulis encrasicolus*) larvae along the Catalan continental slope (NW Mediterranean). *Fisheries Oceanography* 16, 130–141.
- Sawada, Y., Okada, T., Miyashita, S., Murata, O., Kumai, H., 2005. Completion of the Pacific bluefin tuna *Thunnus orientalis* (Temminck et Schlegel) life cycle. *Aquaculture Research* 36, 413–421.
- Schar, C., Vidale, P.L., Luthi, D., Frei, C., Haberli, C., Liniger, M.A., Appenzeller, C., 2004. The role of increasing temperature variability in European summer heatwaves. *Nature* 427, 332–336.
- Sparnocchia, S., Schiano, M.E., Picco, P., Bozzano, R., Cappelletti, A., 2006. The anomalous warming of summer 2003 in the surface layer of the Central Ligurian Sea (Western Mediterranean). *Annales Geophysicae* 24, 443–452.
- Teo, S.L.H., Boustany, A., Dewar, H., Stokesbury, M.J.W., Weng, K.C., Beemer, S., Seitz, A.C., Farwell, C.J., Prince, E.D., Block, B.A., 2007. Annual migrations, diving behavior, and thermal biology of Atlantic bluefin tuna, *Thunnus thynnus*, on their Gulf of Mexico breeding grounds. *Marine Biology* 151, 1–18.
- Tintore, J., Gomis, D., Alonso, S., Parrilla, G., 1991. Mesoscale dynamics and vertical motion in the Alboran Sea. *Journal of Physical Oceanography* 21, 811–823.
- Vargas-Yañez, M., Plaza, F., Garcia-Lafuente, J., Sarhan, T., Vargas, J.M., Velez-Belchi, P., 2000. About the seasonal variability of the Alboran Sea circulation. *Journal of Marine Systems* 35, 229–248.
- Velez-Belchi, P., Tintore, J., 2001. Vertical velocities at an ocean front. *Scientia Marina* 65, 291–300.
- Vilibic, I., Orlic, M., 2000. Adriatic water masses, their rates of formation and transport through the Otranto Strait. *Deep-Sea Research I* 49, 1321–1340.
- Visser, A.W., 1997. Using random walk models to simulate the vertical distribution of particles in a turbulent water column. *Marine Ecology Progress Series* 158, 275–281.
- Werner, F.E., MacKenzie, B.R., Perry, R.I., Lough, R.G., Naimie, C.E., Blanton, B.O., Quinlan, J.A., 2001. Larval trophodynamics, turbulence, and drift on Georges Bank: a sensitivity analysis of cod and haddock. *Scientia Marina* 65 (Suppl. 1), 99–115.
- Young, J.W., Davis, T.L.O., 1990. Feeding ecology of larvae of southern bluefin, albacore and skipjack tunas (Pisces: Scombridae) in the eastern Indian Ocean. *Marine Ecology Progress Series* 61, 17–29.